



Multi-objective optimization for sustainable turning Ti6Al4V alloy using grey relational analysis (GRA) based on analytic hierarchy process (AHP)

Muhammad Younas¹ · Syed Husain Imran Jaffery¹ · Mushtaq Khan¹ · Muhammad Ali Khan¹ · Riaz Ahmad¹ · Aamir Mubashar¹ · Liaqat Ali²

Received: 19 June 2019 / Accepted: 13 August 2019 / Published online: 27 August 2019
© Springer-Verlag London Ltd., part of Springer Nature 2019

Abstract

Sustainable machining necessitates energy-efficient processes, longer tool lifespan, and greater surface integrity of the products in modern manufacturing. However, when considering Ti6Al4V alloy, these objectives turn out to be difficult to achieve as titanium alloys pose serious machinability challenges, especially at elevated temperatures. In this research, we investigate the optimal machining parameters required for turning of Ti6Al4V alloy. Turning experiments were performed to optimize four response parameters, i.e., specific cutting energy (SCE), wear rate (R), surface roughness (R_a), and material removal rate (MRR) with uncoated H13 carbide inserts in the dry cutting environment. Grey relational analysis (GRA) combined with the analytic hierarchy process (AHP) was performed to develop a multi-objective function. Response surface optimization was used to optimize the developed multi-objective function and determine the optimal cutting condition. As per the ANOVA, the interaction of feed rate and cutting speed ($f \times V$) was found to be the most significant factor influencing the grey relational grade (GRG) of the multi-objective function. The optimized machining conditions increased the MRR and tool life by 34% and 7%, whereas, reducing the specific cutting energy and surface roughness by 6% and 2% respectively. Using Taguchi-based GRA by analytic hierarchy process (AHP) weights method, the benefits of high-speed machining Ti6Al4V through multi-response optimization were achieved.

Keywords Sustainable machining · Ti6Al4V alloy · Multi-objective optimization · Grey relational grade · Analytic hierarchy process

Abbreviations

AHP	Analytic hierarchy process
ANOVA	Analysis of variance
d	Depth of cut
f	Feed (mm/rev)
GRA	Grey relational analysis
GRC	Grey relational coefficients
GRG	Grey relational grade

MOO	Multi-objective optimization
MRR	Material removal rate
R	Wear rate
R_a	Surface roughness
RSM	Response surface methodology
SCE	Specific cutting energy
TOPSIS	The technique for order of preference by similarity to ideal solution
V	Cutting speed
VB	Flank wear
HSM	High-speed machining

✉ Muhammad Younas
muhammadyounas.phd@smme.nust.edu.pk

¹ Department of Design and Manufacturing Engineering (DME), School of Mechanical and Manufacturing Engineering (SMME), National University of Sciences and Technology (NUST), Sector H-12, Islamabad 44000, Pakistan

² University of Technology Nowshera, Amangarh 24100, Nowshera 24100, KPK, Pakistan

1 Introduction

Machining processes require careful utilization of resources in modern manufacturing. In aerospace products, high-speed machining is preferred as opposed to conventional cutting

speeds because of the numerous advantages associated with high-speed machining [1, 2]. Titanium is extensively used in key manufacturing applications such as aerospace, biomedical, and automotive industries due to its attractive strength properties [3]. However, its machining is challenged by the tool wear at high speed that affects other machining characteristics. As compared with the machining of ferrous alloys where tool-workpiece interaction is more mechanical in nature, the chemical reactivity of titanium makes the tool-workpiece interaction more reactive and chemical in nature [4–6]. The high chemical reactivity of titanium with most tool materials at a temperature over 500 °C, high cutting temperature, work hardening, high cutting pressure, and vibrations make it a difficult to machine material [7]. Table 1 summarizes the mechanical properties of other aerospace alloys vis-à-vis Ti6Al4V. Improvement in the machining features of titanium-based alloys is, therefore, a major concern for researchers worldwide. In modern sustainable manufacturing setup, the three uncompromising machining scopes include productivity, quality, and energy [10]. Economic and environmental benefits of machining can be achieved by reducing the energy consumption of the machine tool [11] and tool wear [12] as it is reported that 90% of the environmental burden is because of electrical energy consumption [13].

The sustainable goal of machining titanium (with longer tool life, minimum energy consumption, and higher material removal rate) can be attained using multi-objective optimization (MOO). Several MOO techniques have been used in optimizing the machining responses as it provides a tradeoff between multiple conflicting responses such as cutting energy, energy efficiency, material rate, surface roughness, and machining time. Nevertheless, these approaches are mostly influenced by Taguchi's method. For instance, Nguyen et al. [14] optimized multiple responses (micro-hardness of machined surface, material removal rate, and surface roughness) in electro-discharge machining using Taguchi and TOPSIS method. Camposeco-Negrete et al. [15] reported optimized

results for energy consumption, MRR, and Ra applying desirability analysis. Ramesh et al. [16] reported response surface optimization for surface roughness analysis in machining titanium alloys using a round tool under various cutting condition. The combined procedure with GRA, RSM, and fuzzy TOPSIS were used by Gok et al. [17] for minimizing surface roughness and cutting forces in the turning process. More recently, principal component and regression analysis were used to develop a trade-off model relating process time, energy consumption, and carbon emission [18]. In another study for optimizing MRR, Ra, and SCE in machining Al6061, Warsi et al. [19] employed Taguchi-based RSM method. In his research, weights to the responses were assigned using the analytic hierarchy process (AHP). Some studies [20] have also reported notch wear, surface roughness, and flank wear considering cutting fluid. Owing to the machinability challenges offered by titanium, research on energy consumption, and wear optimization of hard to cut material like titanium alloys have not been considered by previous researchers.

Many researchers have also reported analysis of optimizing various machining indices for titanium alloys in relation to different cutting conditions and machining environments. But dry machining is the most sustainable option because of its environment-friendliness as well as cost-effectiveness [21]. In a single objective study to optimize surface roughness during high-speed machining (HSM) of Ti6Al4V, better surface integrity was achieved with high MRR via HSM [22]. It was also reported that the depth of cut mostly influences Ra when machining at high speed. Techniques such as particle swarm optimization [23] for milling parameters, predictive modeling using neural networks for roughness and tool wear [24], GRA analysis for optimizing power and MRR in milling [25], and single objective as well as multi-objective optimization of wear, power, and cutting temperature using Taguchi methods have been reported [26–28] for machining Ti6Al4V alloy. However, no analysis for relating tool life, specific cutting energy, MRR, and surface roughness has been reported in

Table 1 Mechanical properties of Ti6Al4V in comparison with other aerospace alloys [8, 9]

Property	Material						
	Titanium	Ti6Al4V	Ti6Al6V-2Sn	Ti-10V-2Fe-3Al	Inconel 718	Al 7075-T6	Al6061-T6
Density (g/cm ³)	4.5	4.43	4.54	4.65	8.22	2.81	2.7
Hardness (HV)	180–184	285–342	361	303	361–438	~ 175	104
Ultimate tensile strength (MPa)	220	950	1050	970	1350	572	310
Yield strength (MPa)	140	880	980	900	1170	503	275
Modulus of elasticity (GPa)	116	113.8	110	110	200	71.7	69
Ductility (%)	54	14	14	9	16	11	12–14
Fracture toughness (MPa m ^{1/2})	70	75	60	–	96.4	20–29	–
Thermal conductivity (W/mK)	17	6.7	6.6	7.8	11.4	130	167
Max. operating temperature (°C)	~ 150	315	315	315	650	–	–

previous research to the author's knowledge. This research focuses on the detailed analysis of these four important responses in turning Ti6Al4V alloy; besides, this investigation is critical as it helps to achieve sustainable goals of manufacturing products. Additionally, most multi-objective optimization studies have assigned equal weight to optimize the machining responses under the study, however, practically, weights can be assigned based on process or industry requirements [29]. While relating different methods of weight assignment to the machining responses, it has been reported that AHP process yields better results compared to equal weights and can provide a realistic approach for improving the material rate and optimizing energy consumption in turning process. Therefore, the AHP method was also used in this research to assign weights using response surface methodology and grey relational analysis to maximize MRR and minimize Ra, R, and SCE. Using the proposed AHP method, sustainable results were also achieved previously for optimization of MRR, Ra, and SCE in turning Al 6061 [19].

2 Research motivation

This research work is mainly focused on multi-response optimization of four responses (SCE, R, Ra, and MRR) during machining Ti6Al4V at various cutting speeds. The methodology in this work is adapted from our previous work on Al 6061 [19], where, important response parameters (SCE, Ra, and MRR) were improved using response surface methodology (RSM) together with analytic hierarchy method (AHP). The research reported a 5% reduction in energy consumption and a 33% improvement in MRR by employing the ideal machine settings. On the other hand, unlike aluminum, titanium alloys present machinability challenges and tool life deteriorates as machining progresses, thus presenting a strong case for including wear rate into the multi-response study of titanium machining. Although wear maps for Ti6Al4V turning and milling have been developed by Jaffrey et al. [4–7] for various conditions, its machinability analysis in terms of other conflicting responses offers a research gap into the assessment of multi-response study (SCE, MRR, R, and Ra) towards achieving sustainable machining goals in case of Ti6Al4V. The present research has also used AHP process for multi-objective optimization as it is promising in its decisive nature with regards to the energy consumption, productivity improvement (maximizing MRR and minimizing Ra) and meeting cleaner production (minimizing SCE and R) goals of benefiting the industry. While it may be argued that MRR may be calculated analytically, its inclusion in the factor analysis is necessary to incorporate the level of productivity while considering the effect of feed, speed, and depth of cut on tool wear and energy. Thus not considering the effect of increasing MRR with increasing feed and speed will downplay the requirement towards enhanced productivity. Also since

MRR has been widely considered as a reliable indicator for productivity by past researchers, the current study incorporates MRR in factor analysis so that continuity with previous research is preserved [4–6]. Future research is being planned to aim at establishing a productivity term which is not dependent on feed speed and depth of cut during machining.

3 Experimental details

The Ti6Al4V bar was used as workpiece material in this study. Chemical compositions of the alloy are shown in Table 2. Experiments for turning were conducted under dry conditions using H13 grade uncoated plain inserts (CCMW 09 T3 04 Rhombic in shape with 0° rake angle and without a chip breaker) provided by Sandvik. Figure 1 shows the experimental arrangement for turning operation on a CNC machine (ML-300). This machine had a spindle power of 26 kW with a maximum rpm of 3300. The machining conditions with their levels are presented in Table 3. These levels of parameters (cutting speed, feed, and depth of cut) were selected based on previous literature [30] and tool manufacturer-recommended operating ranges (Depth of cut, 0.01–4.5 mm; feed rate, 0.01–0.26 mm/rev; cutting speed, 45–180 m/min) [31]. Experiments were repeated two times for data repeatability using a fresh insert in each experimental run.

3.1 Machining responses

Four response parameters studied in this work includes specific cutting energy, wear rate, surface roughness, and material removal rate of the workpiece material. For measuring the power consumed during machining, Yokogawa (CW-240) Analyzer was used directly at the supply of the machine. The power analyzer can measure the power at an interval of 0.1 sec. SCE was measured by dividing the recorded power over the material removal rate (MRR) using Eqs. (1) and (2). This methodology is adapted from previous work [2, 9, 32] for evaluating SCE during machining aluminum.

$$\text{SCE} = P_{\text{cut}} / \text{material removal rate} (v \times f \times d) \quad (1)$$

$$\text{Where } P_{\text{cut}} = P_{\text{actual}} - P_{\text{air}} \quad (2)$$

P_{actual} is the power utilized during the actual cutting time and P_{air} corresponds to the power when an air cut was made.

Table 2 Chemical composition of the alloy (Ti6Al4V)

Ti	V	Al	Fe	Cu	Cr
89.44	4.2	5.7	0.15	0.003	0.0023

Fig. 1 Experimental setup used for turning



It is important to mention here that energy calculations that do not exclude machine-tool-specific parameters would hamper the universal implementation of the research on energy consumption in machining. For this reason, SCE rather than cutting power was used in our analysis. It has earlier been established that SCE is independent of a particular machine tool being used as it is calculated by [30, 32], effectively discounting electrical and mechanical inefficiencies, temperature effects, etc. since the air cut and actual cut are carried out on the same machine at the same environmental conditions. Furthermore, machine tool independence was confirmed by repeating selected experiments on different machine tools.

Optical microscope was used to measure the tool wear of the insert used in each cutting condition. The tool wear was measured according to ISO standard 3685-1993 [33] for single-point turning, detailed in Fig. 2. The flank wear (VB) was normalized over the cutting length to estimate wear rate (R) using Eq. (3) as reported for the development of wear map [7]. A greater negative value of R represents low tool wear and vice versa.

$$R = \log \left[\frac{VB}{l_s} \right] = \left[\frac{VB}{1000tV_c} \right] \quad (3)$$

Table 3 Cutting parameters with their levels

Parameters	Level 1	Level 2	Level 3
Cutting speed (m/min)	50	100	150
Feed (mm/rev)	0.12	0.16	0.2
Depth of cut (mm)	1	1.5	2

Here VB shows the flank wear, l_s is the spiral length of the cut, t is the cutting time, and V_c is the cutting velocity in m/min. The actual machining time (t) in turning can be related to the cutting conditions using Eq. (4)

$$t = \left[\frac{\pi D l}{1000 f V_c} \right] \quad (4)$$

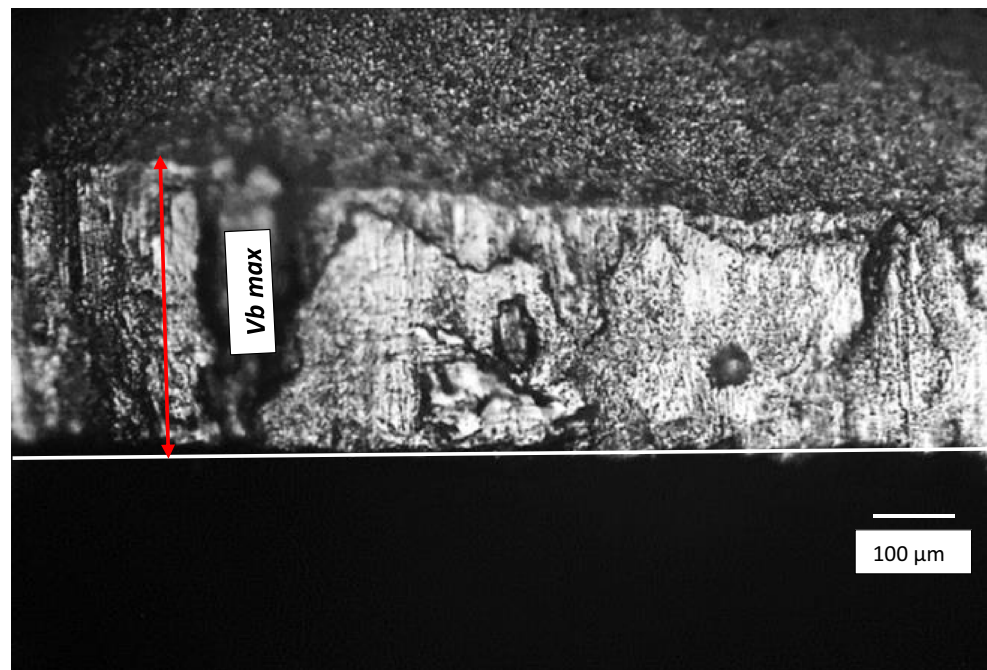
Times TR 100, surface roughness tester was used to take three measurements of roughness value for each machining condition and material removal rate was measured using standard relationships.

3.2 Design of experiments

Using Taguchi experimental design L_9 (3^3) array with nine rows and three columns, turning experiments shown in Table 4 were carried out. The response for each cutting condition represents a mean value of each response repeated two times to minimize error in the experimental data. In this research, each response parameter is first individually analyzed from main effect plots and then response surface methodology is used to statistically optimize multiple responses under varying input parameters. Grey relational function was obtained using AHP weight method and a regression model was developed for the GRG. Lastly, the model is validated for the optimized condition obtained from the analysis.

3.3 Experimental data analysis

The data obtained for the response parameters (SCE, R , Ra, and MRR) was analyzed to assess the effect of cutting conditions (v , f , and d) on these responses. Figure 3 (a–d) shows the

Fig. 2 Optical image showing flank wear measurement

trend of each response parameter in the main effect plot. The trend observed for SCE is different from aluminum alloys [19] when plotted against the cutting speed. This is because titanium, AISI 4340 steel, and 718Plus Ni-based alloy at high speed results in severe tool wear as opposed to aluminum machining that affects the cutting forces and the corresponding cutting energies [34–36]. The progressive tool wear, the strain hardening at high speed, as well as material adhesion at the cutting edge of the tool, result in high values of SCE when machining at high speeds [30]. Titanium is well known to exhibit these attributes [5, 37]. The effect of material adhesion was shown to have increased the value of SCE in the machining Al6061-T6 alloy in a specific region characterized by high SCE [2]. Although cutting force analysis can be found in the literature [38], the trend for SCE is unique and has not been reported earlier to the awareness of the authors. The detailed analysis of SCE regarding the mechanics of chip formation and cutting forces will be presented in the follow-up publication. From

Fig. 3, it can be observed that the SCE, R , and MRR increases and Ra decrease with an increase in the cutting speed. Whereas, increasing the feed rate decreases the SCE and increases Ra, R , and MRR. The trend for the depth of cut for all the four responses is almost the same.

Best responses for Ra and MRR were achieved at high speed (150 m/min), whereas at high depth of cut (2 mm), best values of SCE, Ra, and MRR were attained. Worst values of Ra and R were achieved at higher feed rates because the tool vibration increases at high feed rates resulting in high wear rate and surface roughness values [39]. The best and worst responses for all the experimental runs are given in Table 5. The tool flank wear in an SEM micrograph (shown in Fig. 4) represents the best and worst condition, where the wear remained within the limit of 0.3 mm as specified by ISO. It is evident that different settings of the machine are required to achieve the best response of SCE, R , Ra, and MRR. The wear rate and SCE are best at low speed, whereas Ra and MRR are

Table 4 Experiments using the L9 orthogonal array and their responses

Exp #	f (mm/rev)	V (m/min)	d (mm)	SCE (J/mm^3)	Wear rate, R	Ra (μm)	MRR (cm^3/s)
1	0.12	50	1	1.00	− 6.14	1.113	0.09996
2	0.12	100	1.5	1.33	− 5.84	1.210	0.29988
3	0.12	150	2	1.21	− 5.58	1.023	0.59976
4	0.16	50	1.5	0.95	− 6.10	1.580	0.19992
5	0.16	100	2	1.18	− 5.83	1.237	0.53312
6	0.16	150	1	1.20	− 5.80	0.843	0.39984
7	0.2	50	2	0.93	− 5.58	2.290	0.3332
8	0.2	100	1	0.99	− 5.81	2.080	0.3332
9	0.2	150	1.5	1.18	− 5.29	1.220	0.7497

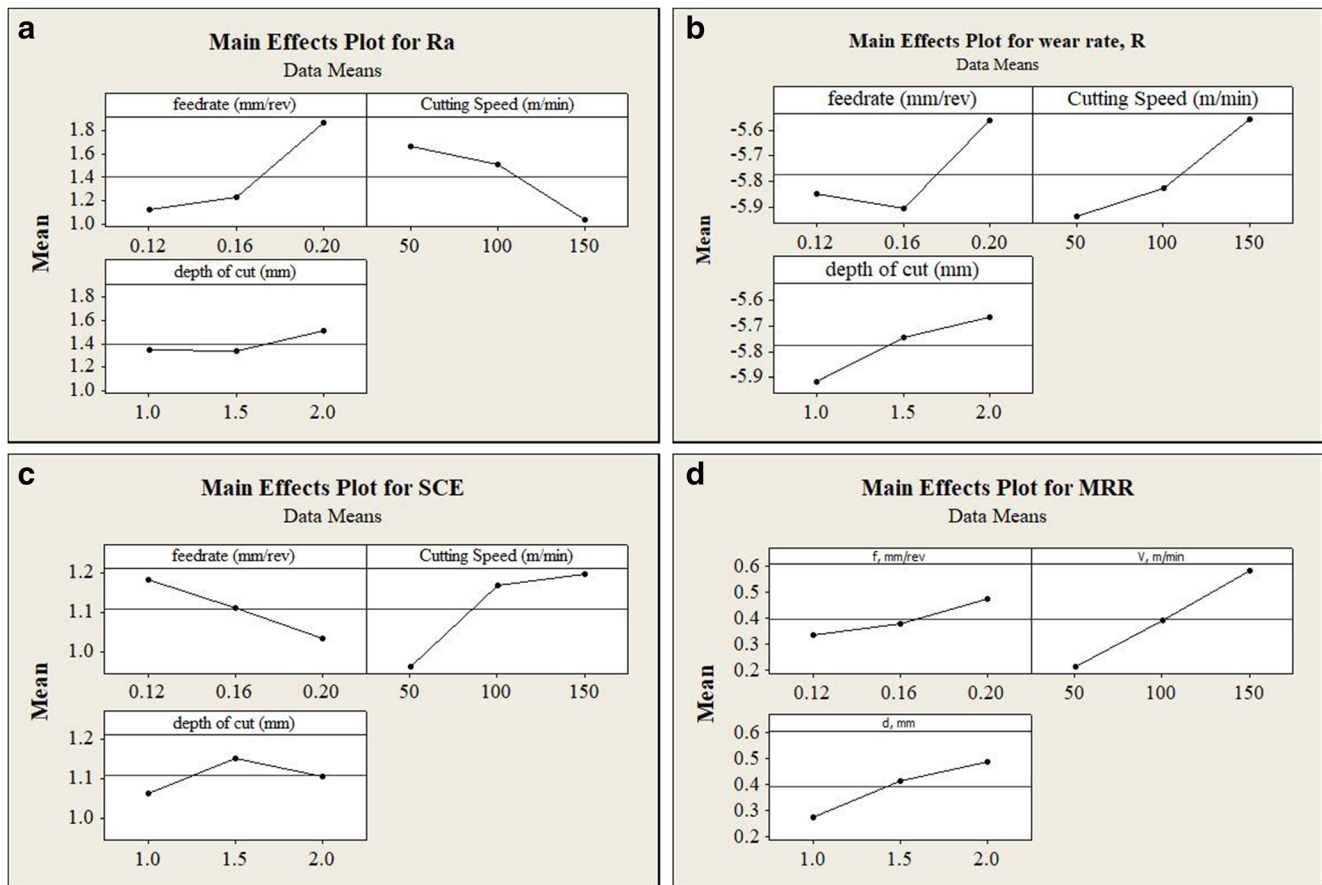


Fig. 3 Main effect plots of response parameters (a) Ra, (b) R, (c) SCE, and (d) MRR

best at high speed. Since these settings are different to produce, the best responses, therefore, there is a strong case for decision-making using multi-objective optimization of these responses in turning titanium alloys.

3.4 Grey relational analysis for multi-objective optimization

In machining processes, usually, an improvement in one response is not possible without lessening the other. Multi-objective optimization is very helpful in making difficult decisions where contending responses are involved. The methodology used in this study is adopted from earlier research [19] on multi-objective optimization of three parameters (SCE, MRR, and Ra) during turning Al6061 alloy as shown in Fig. 5. Optimization of the machining parameters was performed using grey relational analysis (GRA) together with the analytic hierarchy process (AHP). GRA based on Taguchi method transforms a multi-response problem into a single unique function [40].

From the literature [19, 29], various steps involved in performing GRA are given as follows:

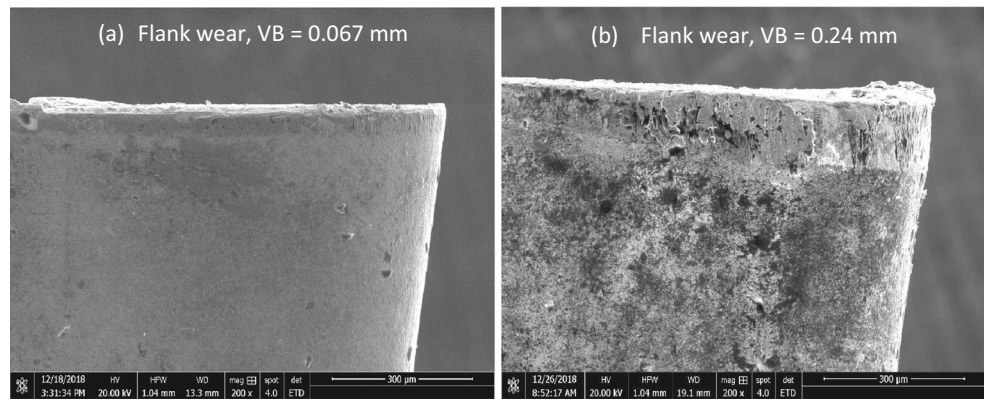
4 Data preprocessing

GRA starts by converting each response to a common scale (0–1) by normalizing all the responses. Normalization of the responses depends on the particular objective. Specific cutting energy (SCE), wear rate (R), and surface roughness (Ra) is to be minimized, whereas material removal rate (MRR) is to be maximized in this research work. Thus, the experimental results for four responses (specific cutting energy, wear rate,

Table 5 The best and worst responses obtained from cutting conditions

Responses	Cutting conditions and their levels				
	Average	f (mm/rev)	V (m/min)	d (mm)	
SCE (J/mm^3)	Worst	1.334	0.12	100	1.5
	Best	1.023	0.20	50	2
Wear rate, R	Worst	-5.29	0.2	150	1.5
	Best	-6.14	0.12	50	1
Ra (μm)	Worst	2.29	0.2	50	2
	Best	0.843	0.16	150	1
MRR (cm^3)	Worst	0.0999	0.12	50	1
	Best	0.7497	0.2	150	2

Fig. 4 SEM micrographs showing the results for wear. (a) Best condition and (b) worst condition



surface roughness, and material removal rate) were normalized for the target value. The values for SCE, R, and Ra are estimated as “smaller the better” using Eq. 5, but for MRR, the

purpose was “larger the better” and the sequence is normalized using Eq. 6.

$$Z_{ij} = \frac{\max(y_{ij}, i = 1, 2, \dots, n) - y_{ij}}{\max(y_{ij}, i = 1, 2, \dots, n) - \min(y_{ij}, i = 1, 2, \dots, n)} \quad (5)$$

$$Z_{ij} = \frac{y_{ij} - \max(y_{ij}, i = 1, 2, \dots, n)}{\max(y_{ij}, i = 1, 2, \dots, n) - \min(y_{ij}, i = 1, 2, \dots, n)} \quad (6)$$

Where $\max(y_{ij})$ and $\min(y_{ij})$ represents the maximum and minimum values of the experimental data for each response. Y_{ij} and Z_{ij} represent the true and normalized values respectively.

5 Calculation of grey relational coefficients

The normalized values are then used to calculate the grey relational coefficients (GRC) using Eq. 7. GRC relates the ideal value of the response to the experimental values.

$$\gamma(Z_o, Z_{ij}) = \frac{\Delta_{\min} + \xi \Delta_{\max}}{\Delta_{oj}(k) + \xi \Delta_{\max}} \quad (7)$$

$$0 < \gamma(Z_o, Z_{ij}) \leq 1$$

Δ_{\max} and Δ_{\min} are the largest and smallest value of the deviation sequence. The deviation sequence, $\Delta_{oj}(k)$ in the above equation can be estimated by

$$\Delta_{oj}(k) = \left| \left(Z_o(k) - Z_{ij}(k) \right) \right|$$

Where $Z_o(k)$ and $Z_{ij}(k)$ represents the reference and comparability sequence respectively. In this study, the value of ξ (distinguishing coefficient) is considered 0.5, which can range between 0–1. The values of GRC estimated for the four responses are shown in Table 6.

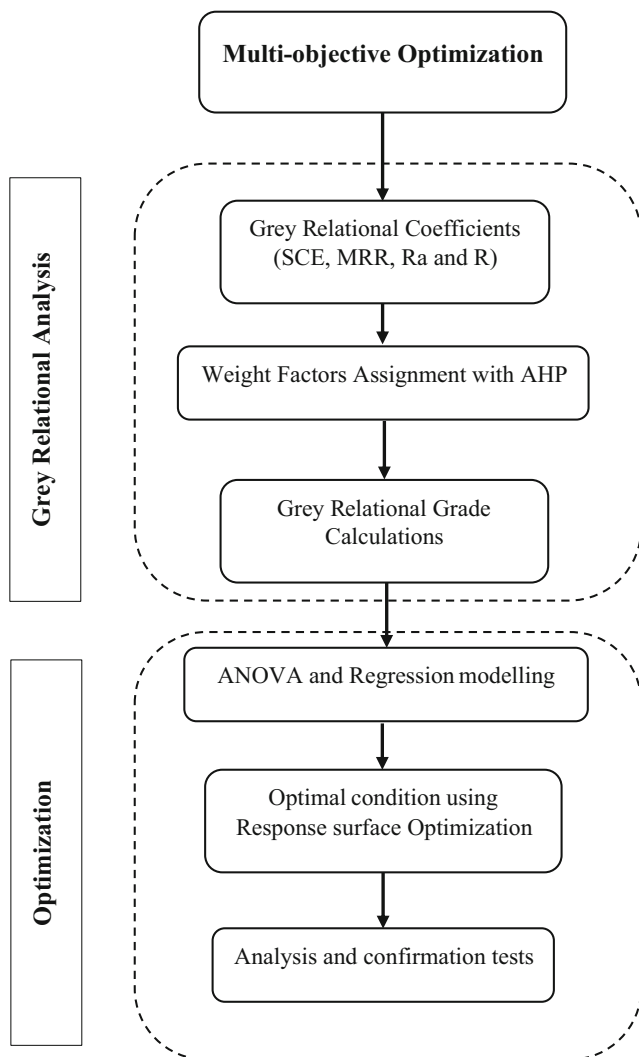


Fig. 5 Methodology for multi-objective optimization

Table 6 GRC and GRG Calculated from the responses

Exp #	<i>f</i> (mm/rev)	<i>V</i> (m/min)	<i>d</i> (mm)	Grey relational coefficients				
				GRC (<i>R</i>)	GRC (Ra)	GRC (SCE)	GRC (MRR)	GRG
1	0.12	50	1	1.0000	0.7282	0.7423	0.3333	0.568425887
2	0.12	100	1.5	0.5864	0.6636	0.3333	0.4194	0.459698809
3	0.12	150	2	0.4312	0.8007	0.4201	0.6842	0.597839368
4	0.16	50	1.5	0.9152	0.4954	0.9098	0.3714	0.580347865
5	0.16	100	2	0.5772	0.6478	0.4453	0.6000	0.574590477
6	0.16	150	1	0.5564	1.0000	0.4276	0.4815	0.527577671
7	0.2	50	2	0.4313	0.3333	1.0000	0.4382	0.516452827
8	0.2	100	1	0.5672	0.3690	0.7707	0.4382	0.512326514
9	0.2	150	1.5	0.3333	0.6576	0.4465	1.000	0.746295296

6 Calculation of GRG

Grey relational grade (GRG) converts the multiple GRC into a combined factor using the assigned weight value of each response. Equation (8) is used to compute weighted GRG. This research used a developed AHP method for weight assignment to four responses under study.

$$\text{Grade } (Z_o, Z_{ij}) = \sum_{k=1}^n \omega_k \gamma(Z_o, Z_{ij}) \tag{8}$$

$$\sum_{k=1}^n \omega_k = 1 \tag{9}$$

7 Weight factors using the analytic hierarchy process (AHP)

Weights in this study were assigned to the response variables using AHP method as reported by previous researchers. The various steps involved are described below.

- a) The decision maker using AHP method calculates the weight of each response. In the first step, a pairwise matrix ($C_{m \times m}$) [29, 41] is constructed with *m* attributes as shown in Eq. 10, where the Saaty’s 9-point scale (Table 7)

Table 7 Nine-point Saaty’s scale

Scale	Definition	Explanation
1	Equally important	Indifferent
3	Weakly important	Slightly better
5	Strongly important	Better
7	Very strongly important	Much better
9	Extremely important	Definitely much better
2, 4, 6, 8	Intermediate value	When compromise needed

is used to determine the comparative rank of each attribute with respect to the goal. After deciding the relative standing of each attribute pertinent to objective, the elements in the pairwise matrix are fixed as given in Table 8. Here, values of the row attributes are compared with the column attributes. Value of 1 is assigned when an attribute is compared with itself ($c_{ij} = 1$ for $i = j$) and when compared with another attribute, a reciprocal value of the corresponding element is assigned ($c_{12} = 1/c_{21}$). Thus, in this matrix, the diagonal values are all 1 and based on the relative importance of the respective attributes half of the values in the matrix are defined. The left behind half values in the matrix are the reciprocal of their corresponding entries.

$$C_{m \times m} = \begin{matrix} C_1 \\ C_2 \\ C_3 \\ \dots \\ C_i \\ \dots \\ C_m \end{matrix} \begin{bmatrix} 1 & C_{12} & C_{13} & \dots & C_{1j} & \dots & C_{1m} \\ C_{21} & 1 & C_{23} & \dots & C_{2j} & \dots & C_{2m} \\ C_{31} & C_{32} & 1 & \dots & C_{3j} & \dots & C_{3m} \\ \dots & \dots & \dots & \dots & \dots & \dots & \dots \\ C_i & C_{i2} & C_{i3} & \dots & 1 & \dots & C_{im} \\ \dots & \dots & \dots & \dots & \dots & \dots & \dots \\ C_m & C_{m2} & C_{m3} & \dots & C_{mj} & \dots & 1 \end{bmatrix} \tag{10}$$

The objective in this research was to improve productivity as well as quality during turning Ti6Al4V without deteriorating tool life (within the limits of ISO tool life standard) and minimizing energy consumption. Since titanium alloys are

Table 8 The Pairwise matrix comparing attributes

Responses	SCE	R	Ra	MRR
SCE	1	1	3	1/7
R	1	1	3	1/2
Ra	1/3	1/3	1	1/5
MRR	7	2	5	1

considered as difficult to machine materials, maximization of productivity is of primary importance. Thus, MRR was assigned maximum weight. The second most important objective was tool life followed by SCE and Ra. As sustainable machining demands equilibrium between production quality and SCE [10], thus equal values of the attributes were assigned to SCE and *R* in comparison matrix. These attributes were ranked in accordance with the values reported in the literature [19, 29]. Table 8 shows the ranking of these attributes in a pairwise matrix.

- b) The geometric mean method is used to calculate the normalized weight of the attributes. Table 9 shows the geometric mean and normalized weight calculated from the pairwise matrix using Eqs. 11 and 12.

$$GM = \left[\prod_{j=1}^m a_{ij} \right]^{1/m} \tag{11}$$

$$w_j = GM_i / \sum_{i=1}^m GM_i \tag{12}$$

- c) For the pairwise matrix, the consistency index (CI) is evaluated using Eq. (13). The value of λ_{max} was estimated by the summation of relative score column-wise, multiplying with corresponding normalized weights of the attributes and summing the resultants. In this study, the value of λ_{max} came out to be 4.2412 and CI equal to 0.08037.

$$CI = \frac{\lambda_{max} - m}{m - 1} \tag{13}$$

- d) Finally, Eq. (14) was used to calculate the consistency ratio (CR) of the matrix. Table 10 was used to select the random index (RI) for four attributes which is 0.89 for $N = 4$. Thus, CR value in the present research was estimated to be 0.0903. The consistency of the judgment is based on the value of CR obtained from the pairwise matrix and a value of 0.1 or less is usually acceptable

Table 9 Geometric mean and normalized weights of the attributes

Responses	Geometric mean	Normalized weights
SCE	0.8091	0.15
<i>R</i>	1.1066	0.21
Ra	0.3860	0.08
MRR	2.892	0.55

Table 10 Attributes and their random consistency index (RI)

N	1	2	3	4	5	6	7	8	9	10
RI	0	0	0.52	0.89	1.11	1.25	1.35	1.4	1.45	1.49

testifying a good investigation being made about the case in hand.

$$CR = \frac{CI}{RI} \tag{14}$$

7.1 Grey relational grade calculation

A grey relational function (Eq. 15) was determined from the normalized weights (Table 8) by means of AHP. These weights were used to find the GRG of each experimental run shown in Table 6.

$$GRG = 0.15 GRC_{SCE} + 0.21 GRC_R + 0.08 GRC_{Ra} + 0.55 GRC_{MRR} \tag{15}$$

8 Results and discussion

The best value of GRG obtained out of all the cutting conditions was observed for experiment #9 corresponding to parameters ($f = 0.20$ mm/rev, $V = 150$ m/min, and $d = 1.5$ mm). Optimal parameters were then identified by response surface optimization of the calculated GRG values (Table 6) and a regression equation was obtained.

8.1 Regression model for GRG function

A multi-objective function for GRG was developed using a second-order model of RSM, which well fits the GRG obtained from the experimental results. The model equation is shown in Eq. (16) with insignificant terms eliminated from the equation.

$$GRG = 1.29567 - 2.63733 f - 0.0142705 V - 0.0874551 d + 0.0000296 V^2 + 0.0385689 fV + 0.00191444 Vd \tag{16}$$

The applicability of the developed model is only limited to turning Ti6Al4V; using uncoated H13 tools, within the conditions ($50 \text{ m/min} \leq V \leq 150 \text{ m/min}$), ($0.12 \text{ mm/rev} \leq f \leq 0.24$),

and ($1 \text{ mm} \leq d \leq 2 \text{ mm}$), the machine tool and the cutting environment used.

Contour and surface plots of GRG for machining conditions under study are shown in Fig. 6. The surface plots show the interaction of the cutting conditions on the value of GRG obtained. The GRG value in plots is maximum at the highest setting of all the cutting factors as evident from the figure below.

Figure 7 shows the comparison between the values of GRG obtained from the experiments and the developed regression model with a maximum error of 3%. The higher value of GRG for experiment #9 is because of the higher feed rate and depth of cut at a high cutting speed that helped reduce the shear forces along the shear plane with improved MRR and R . The negative effect of high feed rate on R_a is countered by high cutting speed.

8.2 ANOVA for GRG

The statistical analysis was conducted using MINITAB® software, where ANOVA was performed at the 95% confidence level to investigate the significance of the cutting parameters (f , V , and d) as shown in Table 11. The best fit obtained was a

quadratic model indicating high accuracy with $R^2 = 96.8\%$. From the analysis of variance, it was found that the interaction of parameters ($f \times V$ and $V \times V$) is more important in affecting the machining responses and GRG as compared to the individual effect of these parameters (f , V , and d). Among the machining conditions, cutting speed originates as the most influencing factor affecting GRG with contribution ratio of 13.5%, whereas among the interacting factor, ($f \times V$) has the major contribution of 44.5% followed by ($V \times V$) with 21%. Depth of cut and its interaction with other parameters has the least influence among all conditions.

8.3 Optimization of the response surface model for GRG

Response surface optimization was used to get optimal cutting conditions from the model developed in Eq. (16). The optimized results in Fig. 8 shows the maximum GRG value obtained at the highest level of the machine settings ($f = 0.20 \text{ mm/rev}$, $V = 150 \text{ m/min}$, and $d = 2.0 \text{ mm}$). This value is inline with the higher weightage assigned to MRR at 55% as supported by previous researchers [19, 29].

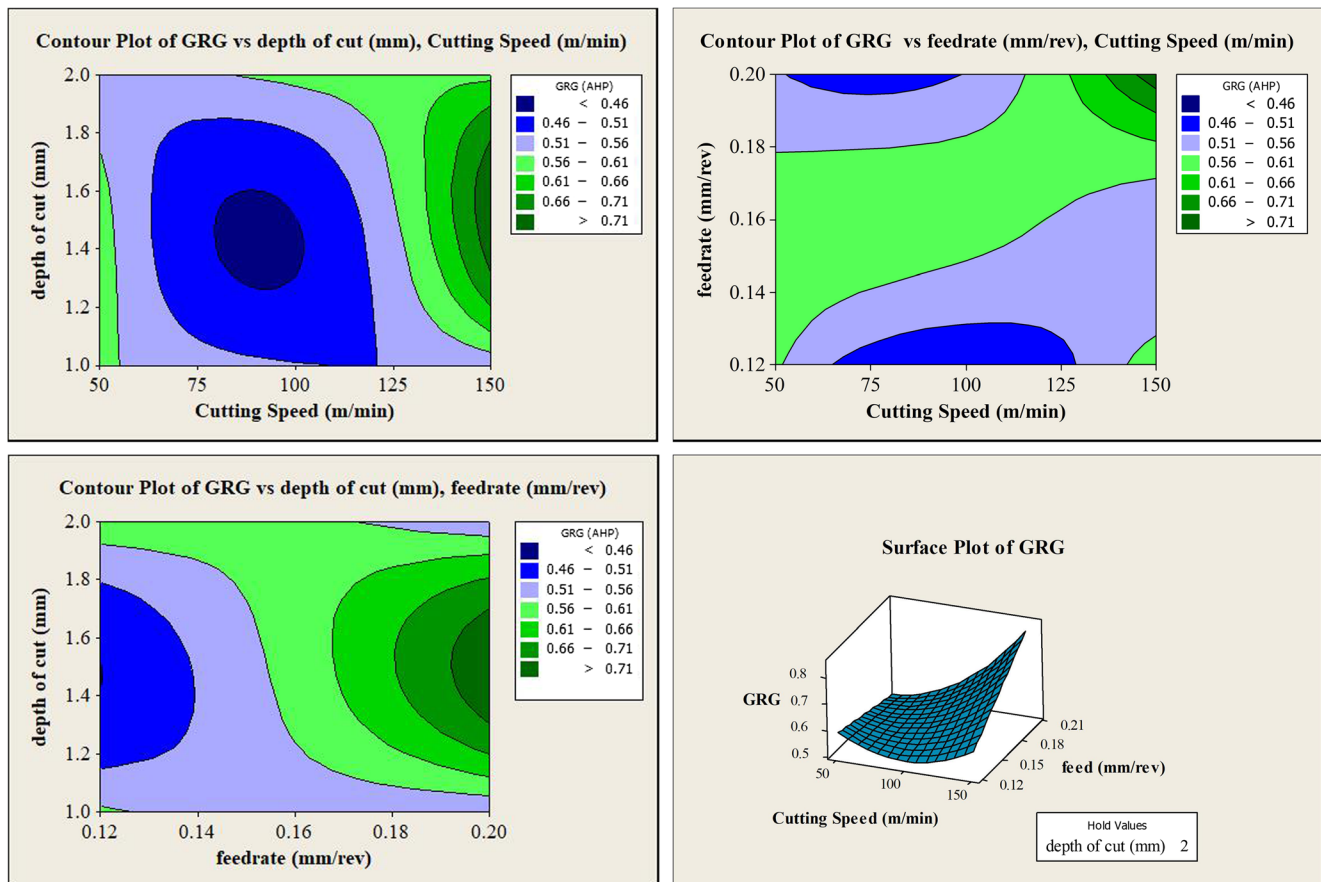
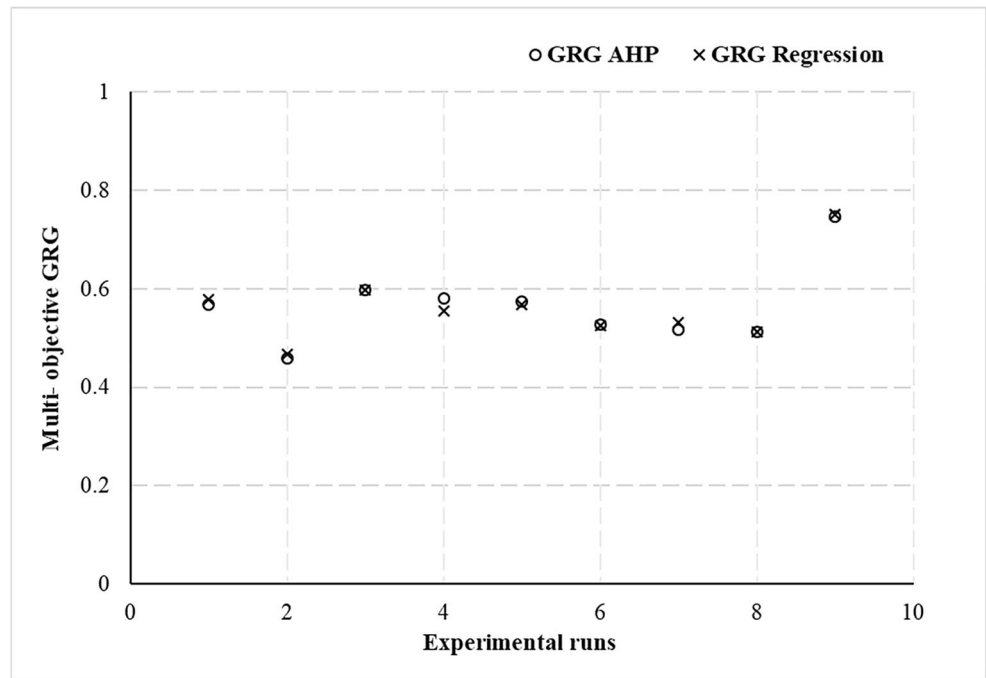


Fig. 6 Surface and contour plots for GRG

Fig. 7 Evaluation of grey relational grade obtained from experiments and calculated from the regression model



8.4 Validation experiments

Table 12 shows the comparison of the optimized machining parameters with the best experimental run (Exp. #9) from the L9 array. The results obtained indicate a 34% increase in MRR, reduction of 6% in the values of specific cutting energy,

and 7% increase in tool life, however, the surface roughness was found to be invariable.

Comparing the best run (Exp. #9) with an optimized run, the only difference in both these conditions is the depth of cut; on the other hand, the cutting speed and feed rate have same values in both the runs. The analysis of machining responses regarding the cutting parameters has a key role in solving multi-objective problems. The MRR increased to 34% in the optimized run because the machine setting is fixed at the highest level for V, f , and d thus resulting in higher MRR. Therefore, MRR is improved if any of the machining condition is increased.

Table 11 ANOVA of GRG

Source	DF	Seq SS	Adj SS	Adj MS	F	CR
Regression	6	0.101634	0.101634	0.016939	85.57	96.8%
Linear	3	0.023786	0.056898	0.018966	95.81	22.3%
F	1	0.007411	0.016658	0.016658	84.15	6.9%
V	1	0.014212	0.014212	0.014212	71.79	13.5%
D	1	0.002163	0.018924	0.018924	95.59	1.9%
Square	1	0.021875	0.021875	0.021875	110.5	20.9%
V*V	1	0.021875	0.021875	0.021875	110.5	20.9%
Interaction	2	0.055972	0.055972	0.027986	141.37	53.5%
f*V	1	0.046351	0.024991	0.024991	126.24	44.5%
V*d	1	0.009621	0.009621	0.009621	48.6	9.1%
Residual	11	0.002178	0.002178	0.000198	–	1.5%
Lack-of-Fit	2	0.002178	0.002178	0.001089	–	1.7%
Total	17	0.103811				100%

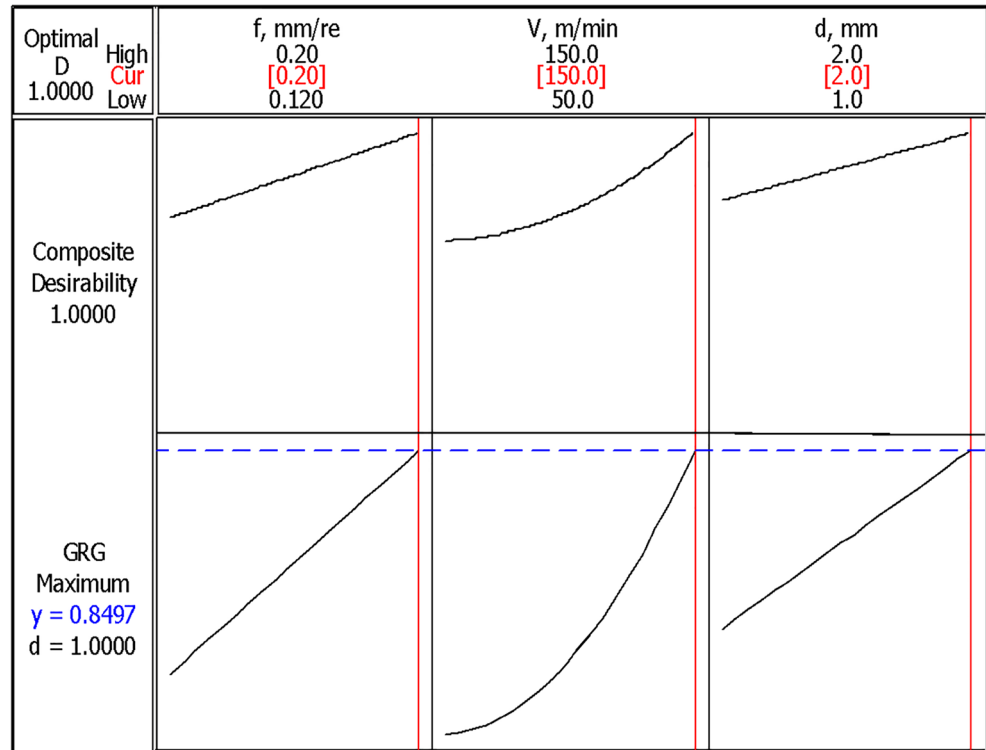
$S = 0.01407$, $R. Sq. (pred) = 95.9$, $R. Sq. (adj) = 96.8$

DOF degrees of freedom, SS sum of squares, MS mean squares, F F value, CR contribution ratio (%), S standard deviation, $R-Sq.(pred.)$ predicted R^2

SCE for optimized run shows a 6% decrease in energy consumption compared to the best run. As the only difference in the two experimental runs (Table 12) is the increase in depth of cut which has resulted in a decrease in SCE values (Fig. 3c), thus endorsing the fact that lower depth of cut values increase the cutting forces and energy consumed at the tooltip [42]. The value of SCE decreases at higher feed rate and increases at high speed, but SCE reduces when both speed and feed is high as evident from ANOVA, ($f \times V$) has the major contribution of 44.5%. This is because at higher feed rate, the mechanics of machining changes to effective shearing rather than rubbing mechanism, reducing the energy consumption at the tooltip [43, 44].

Comparing the surface roughness Ra for the two experimental conditions, higher cutting speed improved the surface integrity of the workpiece because of fewer chances of BUE formation at high speed [45]. Increase in feed rate has also found to worsen the machined surface but higher feed combined with high speed counteracts this negativity. While the

Fig. 8 Responses optimized at maximum GRG



depth of cut has been widely reported to have a minor effect on Ra, thus increase in depth of cut from 1.5 to 2.0 mm in the optimized run has not produced major variations in the values of Ra obtained in this research compared to Exp. #9.

Wear rate (*R*) for both Exp. #9 and optimized experimental run is shown in Table 12. A higher negative value of *R* means a longer tool life and vice versa. The tool life was improved by 7% using the optimized conditions. This improvement can be attributed to the decrease in cutting time when machining at high speeds [7] under optimal machining conditions. The tool wear rate was monitored agreeing to the ISO tool life recommendations (flank wear, $VB \leq 0.3$), therefore, in all the tests, the maximum tool wear reached was under the ISO recommended values. Thus, the multi-objective optimization example presented here has compensated the tool life with a goal to achieve sustainability and economic production.

Although changing the cutting parameters may have an adverse effect on some response because of their conflicting nature, but optimized multi responses can be achieved using

the right combination of cutting condition, which is of utmost importance in machining industries.

9 Conclusions

With regard to the machining of Ti6Al4V, the key responses that were considered in this study showed a conflicting trend with respect to the input cutting conditions. Optimal parameters were achieved using multi-objective optimization of all these responses to attain the sustainable goal of manufacturing products for aerospace and automotive applications. The following can be concluded from the investigation of the experimental results:

- Multi-objective analysis using GRG helped identify optimal solution by means of AHP weight method. This resulted in a cutting condition that provides a tradeoff between the four conflicting responses. The optimum

Table 12 Optimized run in comparison with the best experimental run

	Machining conditions			Responses			
	<i>f</i>	<i>V</i>	<i>d</i>	SCE	<i>R</i>	Ra	MRR
Best run	0.2	150	1.5	1.180	- 5.29	1.220	0.7497
Optimized run	0.2	150	2	1.114	- 5.67	1.201	0.9996
% change				6% decrease	7% decrease	2% decrease	34% increase

condition that resulted in maximum GRG has a speed of 150 m/min, feed of 0.20 mm/rev, and depth of cut of 2.0 mm. An improvement of 34% was attained in MRR and 7% in tool life compared to the best run of the L9 array. Nevertheless, SCE reduced by 6% and Ra remained unaffected.

- ANOVA results revealed that while machining hard to cut alloys like titanium, the interaction of the cutting conditions is more influential in affecting the machining responses as compared to the effect of the individual parameter. In this study, the interaction of ($f \times V$) was found as the notable element producing variation in the output responses.
- The study showed an improvement in important responses that affect product quality, energy, and economic aspect of machining thus promoting sustainable manufacturing by using the right combination of feed, speed, and depth of cut. While tool life and productivity with minimum energy consumption are the major concerns in machining titanium-based alloys, variation in surface roughness can be compensated in the finish cuts.

The outcome of this work can also be extended:

- To the analyses of chip morphology and the mechanics of machining Ti6Al4V with regard to the cutting energy/forces, where a detailed process map can be developed to ascertain the right choice of machine settings used by mechanists at the shop floor.
- To the machining of other titanium based and superalloys by introducing cutting fluid consumption, tool life under various cutting environments (dry, wet, and cryogenic), as well as adding the cost of tooling.

Compliance with ethical standards

Conflict of interests The authors declare that they have no conflict of interest.

References

1. Tascioglu E, Gharibi A, Kaynak Y (2019) High speed machining of near-beta titanium Ti-5553 alloy under various cooling and lubrication conditions. *Int J Adv Manuf Technol* 102:4257–4271
2. Warsi SS et al (2018) Development and analysis of energy consumption map for high-speed machining of Al 6061-T6 alloy. *Int J Adv Manuf Technol*:1–12
3. Niknam SA, Khettabi R, Songmene V (2014) Machinability and machining of titanium alloys: a review. In: Davim JP (ed) *Machining of Titanium Alloys*. Springer Berlin Heidelberg, Berlin, Heidelberg, pp 1–30
4. Jaffery SHI, Khan M, Sheikh NA, Mativenga P (2013) Wear mechanism analysis in milling of Ti-6Al-4V alloy. *Proc Inst Mech Eng Part B-J Eng Manuf* 227(8):1148–1156
5. Jaffery SHI, Mativenga PT (2012) Wear mechanisms analysis for turning Ti-6Al-4V-towards the development of suitable tool coatings. *Int J Adv Manuf Technol* 58(5-8):479–493
6. Jaffery SI, Mativenga PT (2009) Study of the use of wear maps for assessing machining performance. *Proc Inst Mech Eng Part B-J Eng Manuf* 223(9):1097–1105
7. Jaffery SI, Mativenga PT (2009) Assessment of the machinability of Ti-6Al-4V alloy using the wear map approach. *Int J Adv Manuf Technol* 40(7-8):687–696
8. Jaffery SHI et al (2015) Statistical analysis of process parameters in micromachining of Ti-6Al-4V alloy. *Proc Inst Mech Eng B J Eng Manuf* 230(6):1017–1034
9. Warsi SS et al (2015) Analysis of power and specific cutting energy consumption in orthogonal machining of Al 6061-T6 alloys at transitional cutting speeds. in *ASME 2015 International Mechanical Engineering Congress and Exposition*. American Society of Mechanical Engineers
10. Mia M, Gupta MK, Lozano JA, Carou D, Pimenov DY, Królczyk G, Khan AM, Dhar NR (2019) Multi-objective optimization and life cycle assessment of eco-friendly cryogenic N2 assisted turning of Ti-6Al-4V. *J Clean Prod* 210:121–133
11. Moradnzhad M, Unver HO (2017) Energy consumption characteristics of turn-mill machining. *Int J Adv Manuf Technol* 91(5):1991–2016
12. Venugopal KA, Paul S, Chattopadhyay AB (2007) Growth of tool wear in turning of Ti-6Al-4V alloy under cryogenic cooling. *Wear* 262(9):1071–1078
13. Li W, Kara S (2011) An empirical model for predicting energy consumption of manufacturing processes: a case of turning process. *Proc Inst Mech Eng B J Eng Manuf* 225(9):1636–1646
14. Nguyen H-P, Pham V-D, Ngo N-V (2018) Application of TOPSIS to Taguchi method for multi-characteristic optimization of electrical discharge machining with titanium powder mixed into dielectric fluid. *Int J Adv Manuf Technol* 98(5):1179–1198
15. Camposeco-Negrete C (2015) Optimization of cutting parameters using response surface method for minimizing energy consumption and maximizing cutting quality in turning of AISI 6061 T6 aluminum. *J Clean Prod* 91:109–117
16. Ramesh S, Karunamoorthy L, Palanikumar K (2012) Measurement and analysis of surface roughness in turning of aerospace titanium alloy (gr5). *Measurement* 45(5):1266–1276
17. Gok A (2015) A new approach to minimization of the surface roughness and cutting force via fuzzy TOPSIS, multi-objective grey design and RSA. *Measurement* 70:100–109
18. Zhang H, Deng Z, Fu Y, Lv L, Yan C (2017) A process parameters optimization method of multi-pass dry milling for high efficiency, low energy and low carbon emissions. *J Clean Prod* 148:174–184
19. Warsi SS, Agha MH, Ahmad R, Jaffery SHI, Khan M (2019) Sustainable turning using multi-objective optimization: a study of Al 6061 T6 at high cutting speeds. *Int J Adv Manuf Technol* 100(1):843–855
20. Sarıkaya M, Güllü A (2015) Multi-response optimization of minimum quantity lubrication parameters using Taguchi-based grey relational analysis in turning of difficult-to-cut alloy Haynes 25. *J Clean Prod* 91:347–357
21. Rajemi M, Mativenga P, Jaffery S (2009) Energy and carbon footprint analysis for machining titanium Ti-6Al-4V Alloy. *J Mach Eng* 9(1):103–112
22. Mia M, Khan MA, Rahman SS, Dhar NR (2017) Mono-objective and multi-objective optimization of performance parameters in high pressure coolant assisted turning of Ti-6Al-4V. *Int J Adv Manuf Technol* 90(1):109–118
23. Escamilla-Salazar IG, Torres-Treviño LM, González-Ortiz B, Zambrano PC (2013) Machining optimization using swarm intelligence in titanium (6Al 4 V) alloy. *Int J Adv Manuf Technol* 67(1):535–544

24. Özel T, Karpat Y (2005) Predictive modeling of surface roughness and tool wear in hard turning using regression and neural networks. *Int J Mach Tools Manuf* **45**(4-5):467–479
25. Shen Y, Liu Y, Dong H, Zhang K, Lv L, Zhang X, Zheng C, Ji R (2017) Parameters optimization for sustainable machining of Ti6Al4V using a novel high-speed dry electrical discharge milling. *Int J Adv Manuf Technol* **90**(9):2733–2740
26. Mia M, Khan MA, Dhar NR (2017) High-pressure coolant on flank and rake surfaces of tool in turning of Ti-6Al-4V: investigations on surface roughness and tool wear. *Int J Adv Manuf Technol* **90**(5-8): 1825–1834
27. Mia M, Khan MA, Dhar NR (2017) Study of surface roughness and cutting forces using ANN, RSM, and ANOVA in turning of Ti-6Al-4V under cryogenic jets applied at flank and rake faces of coated WC tool. *Int J Adv Manuf Technol* **93**(1-4):975–991
28. Mia M, Khan MA, Rahman SS, Dhar NR (2017) Mono-objective and multi-objective optimization of performance parameters in high pressure coolant assisted turning of Ti-6Al-4V. *Int J Adv Manuf Technol* **90**(1-4):109–118
29. Kumar R, Bilga PS, Singh S (2017) Multi objective optimization using different methods of assigning weights to energy consumption responses, surface roughness and material removal rate during rough turning operation. *J Clean Prod* **164**:45–57
30. Younas M et al (2019) Tool Wear Progression and its Effect on Energy Consumption in Turning of Titanium Alloy (Ti-6Al-4V). *Mech Sci* **10**(2):373–382
31. Sandvik-Coromant, Product Catalogue, Turning tools. 2015.
32. Warsi SS, Jaffery SHI, Ahmad R, Khan M, Ali L, Agha MH, Akram S (2018) Development of energy consumption map for orthogonal machining of Al 6061-T6 alloy. *Proc Inst Mech Eng B J Eng Manuf* **232**(14):2510–2522
33. ISO, I., 3685 (1993) Tool-life testing with single-point turning tools. International Organization for Standardization (ISO), Geneva, Switzerland
34. Pervaiz S, Deiab I, Darras B (2013) Power consumption and tool wear assessment when machining titanium alloys. *Int J Precis Eng Manuf* **14**(6):925–936
35. Razak NH, Chen ZW, Pasang T (2016) Progression of tool deterioration and related cutting force during milling of 718Plus superalloy using cemented tungsten carbide tools. *Int J Adv Manuf Technol* **86**(9):3203–3216
36. Cho SS, Komvopoulos K (1998) Cutting force variation due to wear of multi-layer ceramic coated tools. *J Tribol* **120**(1):75–81
37. Ezugwu EO, Wang ZM (1997) Titanium alloys and their machinability—a review. *J Mater Process Technol* **68**(3):262–274
38. Sun S, Brandt M, Dargusch MS (2009) Characteristics of cutting forces and chip formation in machining of titanium alloys. *Int J Mach Tools Manuf* **49**(7):561–568
39. Yan J, Li L (2013) Multi-objective optimization of milling parameters – the trade-offs between energy, production rate and cutting quality. *J Clean Prod* **52**:462–471
40. Kuo Y, Yang T, Huang G-W (2008) The use of a grey-based Taguchi method for optimizing multi-response simulation problems. *Eng Optim* **40**(6):517–528
41. Chalisgaonkar R, Kumar J (2015) Multi-response optimization and modeling of trim cut WEDM operation of commercially pure titanium (CPTi) considering multiple user's preferences. *Eng Sci Technol, Int J* **18**(2):125–134
42. Waldorf DJ (2006) A simplified model for ploughing forces in turning. *J Manuf Process* **8**(2):76–82
43. Balogun VA, Edem IF, Adekunle AA, Mativenga PT (2016) Specific energy based evaluation of machining efficiency. *J Clean Prod* **116**:187–197
44. Balogun VA, Mativenga PT (2014) Impact of un-deformed chip thickness on specific energy in mechanical machining processes. *J Clean Prod* **69**:260–268
45. Bahçe E, Ozel C (2013) Experimental investigation of the effect of machining parameters on the surface roughness and the formation of built up edge (BUE) in the drilling of Al 5005, in *Tribology in Engineering*. IntechOpen, London

Publisher's note Springer Nature remains neutral with regard to jurisdictional claims in published maps and institutional affiliations.